Biol. Cybern. 73, 113–121 (1995)

Biological
Cybernetics

# A model of the neuro-musculo-skeletal system for human locomotion

## II. Real-time adaptability under various constraints

**Gentaro Taga**

Department of Pure and Applied Sciences, University of Tokyo, Komaba, Meguro-ku, Tokyo 153, Japan

Received: 29 June 1994/Accepted in revised form: 20 January 1995

**Abstract.** Adaptive gaits of humans were produced as a result of emergent properties of a model based on the neurophysiology of the central pattern generator and the biomechanics of the human musculoskeletal system. We previously proposed a neuromusculoskeletal model for human locomotion, in which movements emerged as a stable limit cycle that was generated through the global entrainment among the neural system, composed of neural oscillators, the musculoskeletal system, and the environment. In the present study, we investigated the adaptability of this model under various types of environmental and task constraints. Using a computer simulation, it was found that walking movements were robust against mechanical perturbations, loads with a mass, and uneven terrain. Moreover, the speed of walking could be controlled by a single parameter which tonically drove the neural oscillators, and the step cycle could be entrained by a rhythmic input to the neural oscillators.

## 1 Introduction

How humans generate locomotor behaviors that adapt to a changing environment is of interest in the interdisciplinary fields of neurophysiology, kinesiology, biomechanics, and robotics. The real-time adaptability of humans when they are confronted with an unpredictable environment is far more flexible than that of the best so-called intelligent machines. For example, we can generate an appropriate movement promptly when the movement of our entire body is disturbed by an unpredictable change in ground condition or when we walk carrying a heavy bag. Such behaviors are generated not merely by a simple reflex mechanism but by a globally organized mechanism for integration of action and perception in real time. Here we shall focus on an emergent property of the neural and musculo-skeletal systems during dynamic interaction with the environment. The purpose of this study is to demonstrate the mechanism for the real-time adaptation of locomotion.

According to the traditional control theory, planning of a trajectory, generation of motor commands, and adaptation by feedback are completely separated. The real-time adaptability is attributed to the feedback control which reduces deviation from a preset trajectory. A system based on such a control principle will be confronted with problems when the environment changes suddenly and it does not have ability to change its desired trajectory and motor command in real time. The control of human-like bipedal robots has been studied based on such feedback and feedforward control using a gait with a prescribed trajectory (Miura and Shimoyama 1984; Takanishi et al. 1990; Furusho and Sano 1991). However, locomotor systems inevitably possess unpredictability due to interaction with the changing environment. It is impossible to directly control the degrees of freedom with which the feet contact the ground (Vukobratovic and Stokic 1975). To adapt to a changing environment in real time, a mechanism which produces a trajectory in real time using the current state of the system is needed.

Taga et al. (1991) proposed an alternative principle of locomotor control in which movements emerge through global entrainment among the rhythmic activity of the neural system, the rhythmic movements of the musculoskeletal system, and interaction with the changing environment. This principle, called global entrainment, was inspired by the neurophysiological mechanism for animal locomotion, in which the interaction between the central pattern generator (CPG) and the sensory system generates normal and adaptive locomotion (Grillner 1985). In terms of nonlinear dynamical theory (Schöner and Kelso 1988), the stability of movement is established as an attractor that is generated through the interaction of neural and effector dynamics. Related models which present motor control systems as two dynamical systems have been studied (Beer 1990; Doya and Yoshizawa 1992; Ekeberg 1993; Kimura et al. 1993; Schöner 1993). In the field of robotics, Raibert has emphasized that the control

---

Part of this paper was done at Yukawa Institute for Theoretical Physics, Kyoto University, Japan system and the controlled system should be designed to work together, sharing responsibility for the behavior that emerges (Raibert 1984; Raibert and Hodgins 1992).

Applying the principle of global entrainment, we proposed a model of neuro-musculo-skeletal system for human locomotion which successfully produced a steady-state of walking movement that could be compared with experimental studies in humans (Taga 1995). In the present paper, we will examine further the adaptability of this model under various conditions. Since the entire model is a completely autonomous system, real-time adaptability can be characterized by the stability and flexibility of locomotion when environmental constraints and/or task constraints change while the internal structure and parameters of the system do not change. We will demonstrate the extent to which stable locomotion is maintained against unpredictable changes in environmental constraints such as mechanical perturbations, loads by mass and uneven terrain profiles. We will also show the availability of a wide range of walking speeds, step lengths, and step cycles, which are attributes of locomotion under various task constraints.

## 2 Outline of the model for human locomotion

The model of the neuro-musculo-skeletal system for human locomotion is outlined below (Taga 1995). It is composed of two dynamical systems: a musculo-skeletal system and a neural system. The musculo-skeletal system is modeled as eight segments with 20 muscles in the sagittal plane. The neural system, referred to as the neural rhythm generator, is composed of seven pairs of neural oscillators which correspond to the joints of the body. The neural rhythm generator produces motor signals to induce muscle torques and receives sensory signals indicating the current state of the musculo-skeletal system and the environment. The time required to transport and process signals in the neural system can be assumed to be negligible compared with the slow dynamics of the generation of locomotor rhythm (Taga 1994). The equations of motion can be written as

$$\dot{\varphi} = \mathbf{p}(\varphi, \mathbf{u}, \mathbf{F}_g) \tag{1a}$$

$$\dot{\mathbf{u}} = \mathbf{q}(\mathbf{u}, \varphi, \mathbf{F}_g, \mathbf{u}_0) \tag{1b}$$

where (1a) and (1b) express the musculo-skeletal and neural dynamics, respectively; $\varphi$ is a generalized coordinate of the musculo-skeletal system; $\mathbf{u}$ is a vector of the state of the neural rhythm generator; $\mathbf{F}_g$ is a vector of ground reaction forces, which determine the environmental constraints; and $\mathbf{u}_0$ is a vector of the inputs from the higher center to the neural rhythm generator, which drive and modulate the activity of the latter.

Since human walking is characterized by displacement of the body's center of gravity (COG) with respect to the center of pressure (COP) of the ground reaction forces, we set the orientation of the vector from the COP to the COG in an earth-fixed coordinate to represent global information and call it the global angle. It can be written as

$$\phi = \cos^{-1}[x_{cp} - x_{cg})/\{(x_{cp} - x_{cg})^2 + (y_{cg} - y_{cp})^2\}^{\frac{1}{2}}] \tag{2}$$

where $(x_{cg}, y_{cg})$ and $(x_{cp}, y_{cp})$ are coordinates of the COG and COP, respectively. An approximation of the first derivative of the global angle with respect to time is called the global angular velocity and described as

$$\dot{\phi} = \{(y_{cg} - y_{cp})\dot{x}_{cg} + (x_{cp} - x_{cg})\dot{y}_{cg}\}/\{(x_{cp} - x_{cg})^2 + (y_{cp} - y_{cg})^2\} \tag{3}$$

Each neural oscillator receives the sensory input regarding the local and global angular information, and the global stability of locomotion is established through global entrainment. In this paper, the global angle and global angular velocity are used as a reduced description of the global behavior of the system.

We examined various types of environmental constraints. Mechanical perturbations are given as instantaneous forces applied to body segments. Load by mass is represented by changes in inertial parameters. Changes in terrain are described by a function of the terrain profile.

Although task constraints are not explicitly represented in this model, inputs from the higher center of the neural system to the neural rhythm generator can modulate the basic gait pattern and produce appropriate behaviors that may fit task constraints. Therefore, we can change the input parameters to examine the models's ability to generate a variety of gaits.

The numerical integration for the differential equations in this model was performed on the HITAC S3800 at the Computer Center of University of Tokyo. Details of the method of calculation have been described in the preceding paper.

## 3 Adaptive walking under changes in environmental constraints

Since the natural environment in which humans move is more complex than can be explicitly represented, it would be impossible for the neural system to have a specific program of movements for each specific disturbance or change to be encountered. Walking without disturbances over level ground was shown in the preceding paper. Here, walking movements under various environmental constraints will be examined.

### *3.1 Mechanical perturbation*

The application of mechanical perturbations to part of the body was examined during walking over level terrain. As a control experiment, Fig. 1A shows a stick figure of the walking movement without disturbances. During the steady-state of walking, impulsive forces were applied to a part of the body at a specific point in the gait cycle. Figure 1B shows a stick figure of the walking movement when a force of 200 N was applied for 0.1 s to the center

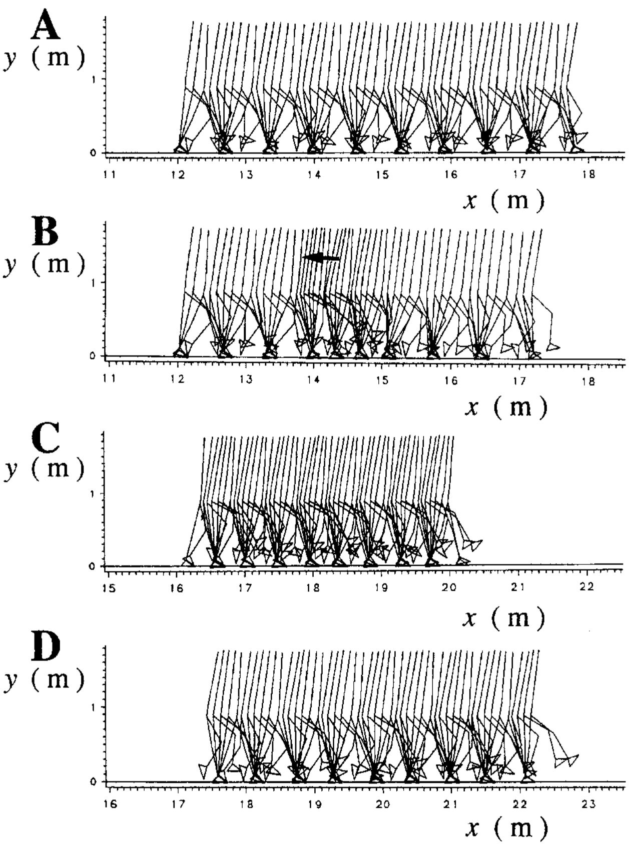

**Fig. 1A–D.** Stick figure of walking movements. The stick figure was traced every 0.09 s. **A** Walking movement in the steady-state. **B** Walking movement when a force of 200 N was applied for 0.1 s to the center of mass of the head, arms, trunk (HAT) in the backward direction. *Arrow* indicates the perturbation. **C** Walking movement when a mass with 15 kg is affixed to the pelvis. The stick figure was shown after the steady-state was reached. **D** Walking movement when a mass with 1.0 kg is affixed to only the right shank. The stick figure was shown after the steady-state was reached

of the HAT (head, arms, and trunk) in the backward direction. After the instantaneous perturbation, the walking pattern was strongly disturbed. However, steady walking was recovered within several step cycles. Figures 2B and 3B show the time courses of the global angle and the global angular velocity, respectively, which clearly demonstrate the strong convergence to the steady-state after the perturbation.

This type of adaptability can be attributed to the orbital stability of the limit cycle that is generated in a state space of the neural and musculo-skeletal variables. When the perturbation is so large that it forces the trajectories to move beyond the separatrix of the stable limit cycle, the model ‘falls down’. Dynamic stability depends on the magnitude and timing of perturbations and the point at which perturbations are applied. In the double-support phase, mechanical perturbations of various magnitudes were applied to various parts of the body in the backward direction for 0.1 s. Maximum values of the perturbations at which stability was maintained were 250 N, 250 N, 200 N and 500 N for the HAT, pelvis, thigh, and shank, respectively. For the HAT and pelvis, the stability against perturbations was similar in the other phases of the gait cycle. However, the effect of perturbations to the limb segments was strikingly different in different phases of the gait cycle. The upper limits of the strength of perturbations to the shank were 500 N, 300 N, 500 N, 40 N, 20 N, and 30 N for the first double-support phase, the first half of the single-support phase, the second half of the single-support phase, the second double-support phase, the first half of the swing phase, and the second half of the swing phase, respectively. Thus, the limb segments possess greater stability against perturbations during the stance phase than during the swing phase.

### *3.2 Load to the body*

We examined walking when a part of the body was loaded by a mass. During the steady walking without a mass, an inertial parameter was assumed to be changed. After several step cycles, a new steady-state was reached. Typical examples of a stick figure of walking movements are shown in Fig. 1C and D. Figure 1C presents a walking movement when a mass of 15 kg was affixed to the pelvis. The step length and speed of walking were less than those during the free walking shown in Fig. 1A. The system could not continue to walk with a mass greater than 20 kg. Figure 1D shows a walking movement when a mass of 1.0 kg was affixed to the right shank. In this case, the speed of walking declined, and an asymmetric gait pattern emerged. Figures 2C, 2D, 3C and 3D show the corresponding displacements of the global angle and global angular velocity, respectively. These figures indicate that the movement of the system converges to a new steady-state, which is slightly different from that of the original limit cycle, according to where the mass was affixed and to the magnitude of the mass. This characteristic means that the limit cycle is structurally stable against changes in inertial conditions within a certain range.

By conducting systematic trials of walking under various conditions of load, we found that the upper limits of the values of mass affixed to the parts of the body were 5 kg, 15 kg, 5 kg, 1 kg, and 0.5 kg for the HAT, pelvis, thigh, shank, and foot, respectively. Therefore, the pelvis is the most stable body part against loading with a mass.

### *3.3 Uneven terrain*

The performance of the system over uneven terrain was examined without applying any additional control that was specific to the profile of the ground. During the steady-state of walking on flat ground, the terrain was assumed to change suddenly. The profile is set up on the sagittal plane such that the height of the terrain changes in the horizontal direction.

We first examined walking on a slope with a constant inclination. The ground profile was described by

$$y_g(x) = \begin{cases} 0 & (x < x_0) \\ a(x - x_0) & (x \geqslant x_0) \end{cases} \tag{4}$$

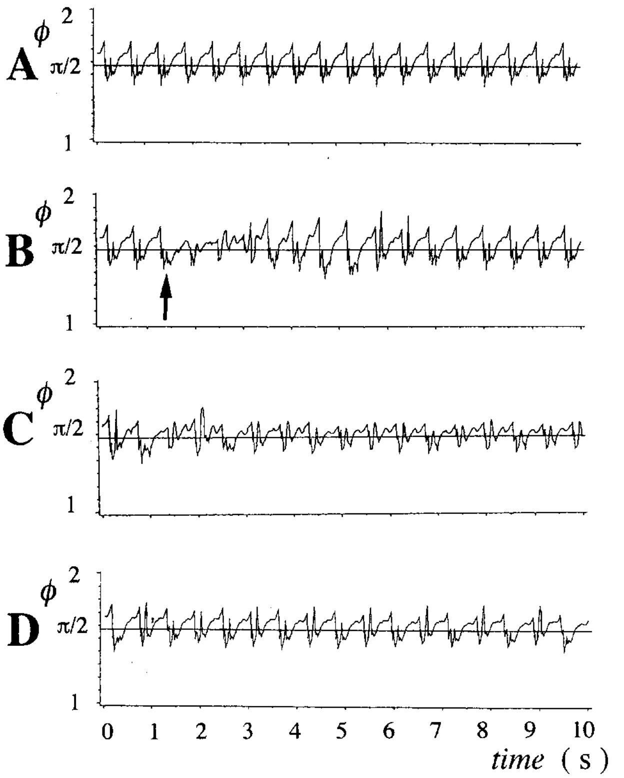

**Fig. 2A–D.** Displacement of the global angle during walking under various conditions. **A** The global angle in the steady state of walking. **B** The global angle when a mechanical perturbation of 200 N was applied for 0.1 s to the center of mass of the HAT in the backward direction. *Arrow* indicates the point at which the perturbation was applied. **C** The global angle when a mass of 15 kg is affixed to the pelvis. **D** The global angle when a mass of 1.0 kg is affixed to only the right shank

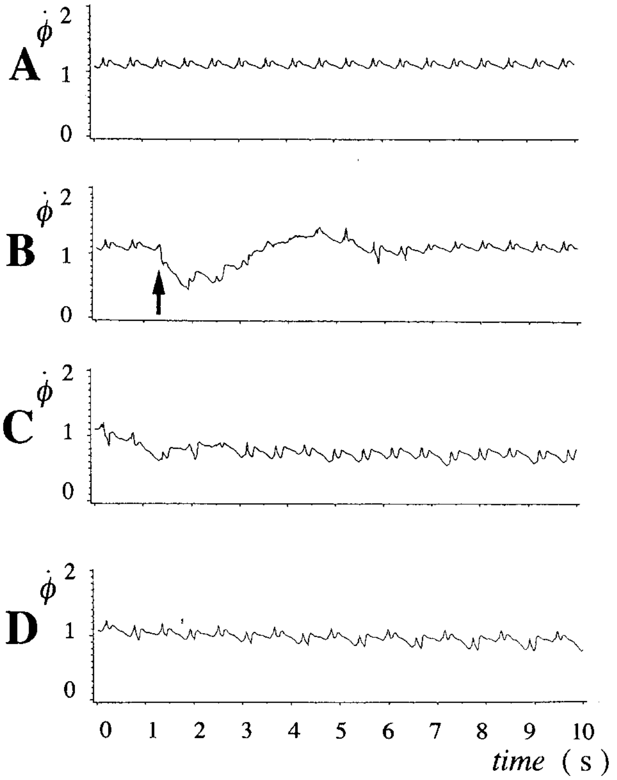

**Fig. 3A–D.** Displacement of the global angular velocity under various conditions. **A** The global angular velocity in the steady-state of walking. **B** The global angular velocity when a mechanical perturbation of 200 N for 0.1 s was applied to the center of mass of the HAT in the backward direction. *Arrow* indicates the point at which the perturbation was applied. **C** The global angular velocity when a mass of 15 kg is affixed to the pelvis. **D** The global angular velocity when a mass of 1.0 kg is affixed to only the right shank

where $a$ is the slope of the terrain and $x_0$ is the position at which the slope of the terrain changes.

Using a computer simulation, stable walking movements were obtained within the limits of the slope; $-0.02 \leqslant a \leqslant 0.02$. Figure 4A shows stick figures of walking movement over ground with $a = 0.02$, 0, and $-0.02$, respectively. Preferred speeds of walking were chosen in a self-organized manner depending on the slope of the terrain. The step length and the walking speed were less going uphill than on flat ground, while they were larger going downhill. Figures 5 and 6 show the corresponding time courses of the global angle and angular velocity, respectively. They demonstrate the changes in the character of the limit cycle, to which the entire system converges.

We next examined walking over a terrain of sinusoidal wave patterns. The profile of the ground was

$$y_g(x) = \begin{cases} 0 & (x < x_0) \\ b \sin \omega (x - x_0) & (x \geqslant x_0) \end{cases} \tag{5}$$

where $b$ is the amplitude of the wave and $\omega$ is a spatial frequency.

Figure 7 shows a typical example of a stick figure of walking movement and the time courses of the global angle and global angular velocity. The global angle and angular velocity change sinusoidally according to the changes in the profile of the ground. The motion does not converge to a steady-state, which contrasts with that on a slope with a constant inclination where a steady-state is reached. We examined walking over various kinds of sinusoidal wave patterns by changing parameters $b$ and $\omega$. Stable walking was obtained when the spatial frequency was sufficiently low and the amplitude was sufficiently small. When the amplitude was 0.02 m, the highest spatial frequency, with which stability was maintained, was 0.8 (wavelength 7.58 m).

## 4 Adaptive walking under changes in task constraints

The availability of a wide range of walking speeds with great stability is an attribute of locomotion under various task constraints. Neurophysiological experiments on quadruped animals have shown that the speed of locomotion and the gait pattern can be controlled by steady electrical stimulation of a region of the midbrain (Shik et al. 1966). This fact suggests that humans may also control walking speed by using information that is non-specific to rhythmic components of walking (Taga et al.

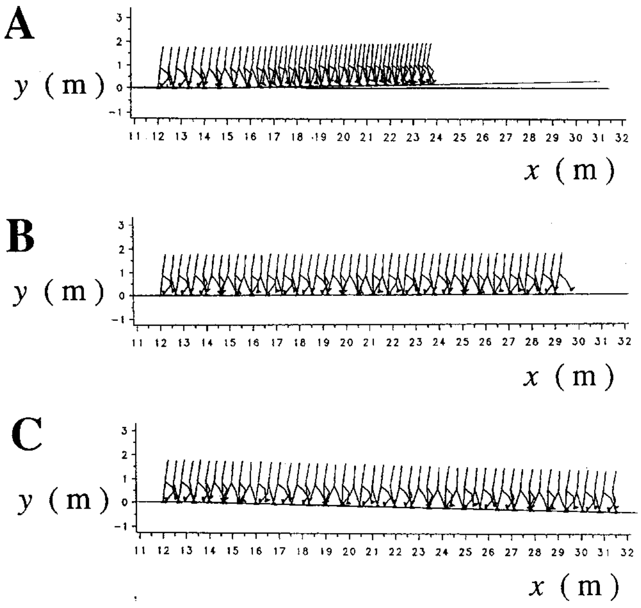

**Fig. 4A–C.** Stick figures of walking movement over a slope. From a steady-state of walking over level ground, the slope changes at $x = 14$. The stick figure was traced every 0.3 s. **A** Uphill with a slope $a = 0.02$. **B** Level ground. **C** Downhill with a slope $a = -0.02$

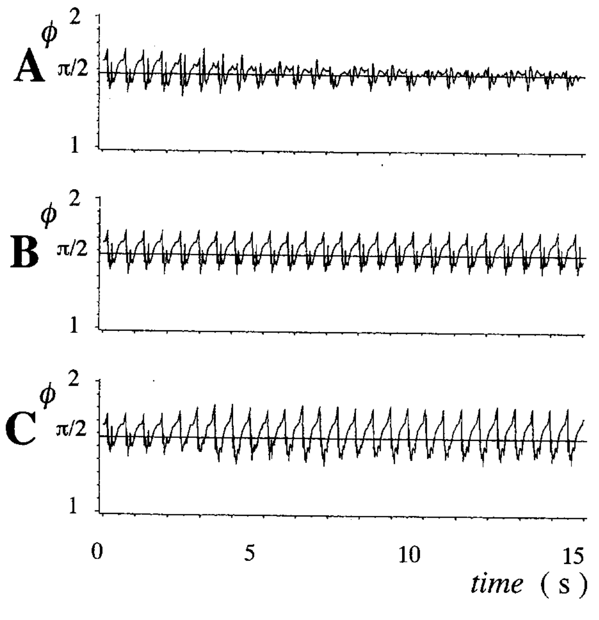

**Fig. 5A–C.** Displacement of the global angle during walking over a slope. **A** Uphill with a slope $a = 0.02$. **B** Level ground. **C** Downhill with a slope $a = -0.02$

1991). On the other hand, humans can control stepping rhythm intentionally; for example, when we synchronize our stepping to a rhythm of music. This control should be based on information that is specific to rhythmic components of locomotion. We show here that modulatory inputs to the neural rhythm generator produce a variety of walking movements.

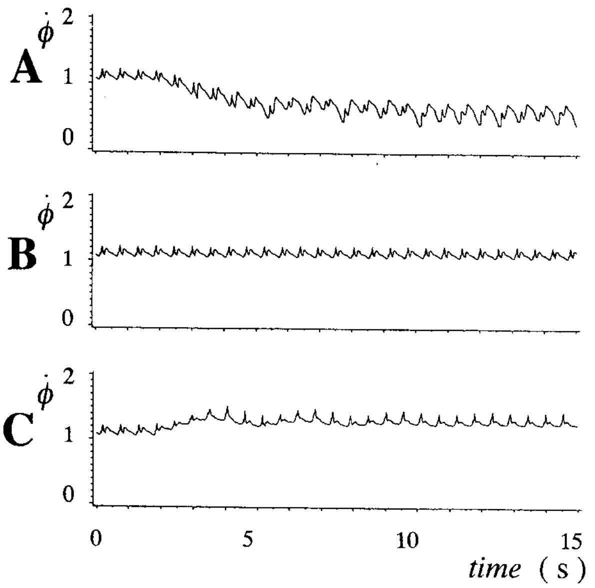

**Fig. 6A–C.** Displacement of the global angular velocity during walking over a slope. **A** Uphill with a slope $a = 0.02$. **B** Level ground. **C** Downhill with a slope $a = -0.02$

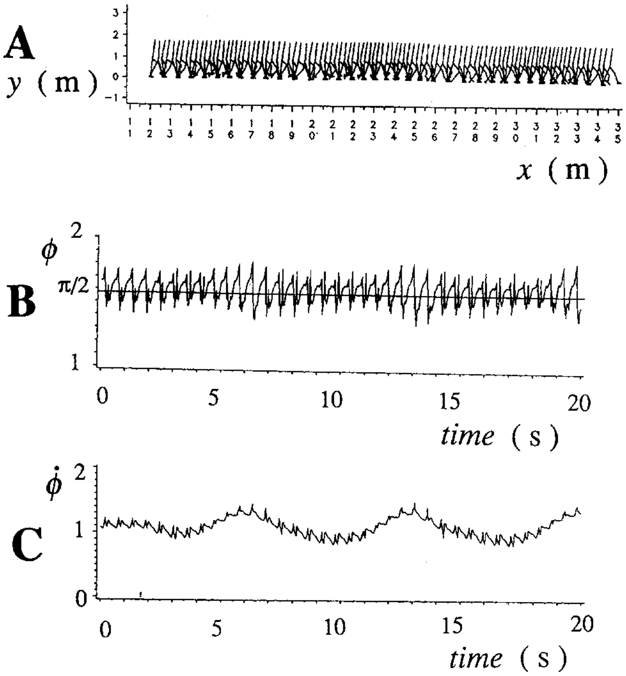

**Fig. 7A–C.** Walking over terrain with a sinusoidal wave pattern. **A** Stick figure of the walking movement. From a steady-state of walking over level ground, the ground profile changes at $x = 14$ to a sinusoidal pattern with $b = 0.02$ and $\omega = 0.8$. The stick figure was traced every 0.2 s. **B** Displacement of the global angle. **C** Displacement of the global angular velocity

### *4.1 Change in walking speed by nonspecific input to the neural rhythm generator*

We examined changes in the input parameter $u_0$ which drove the activity of each neural oscillator tonically and induced nonspecific changes in muscle torques. Walking

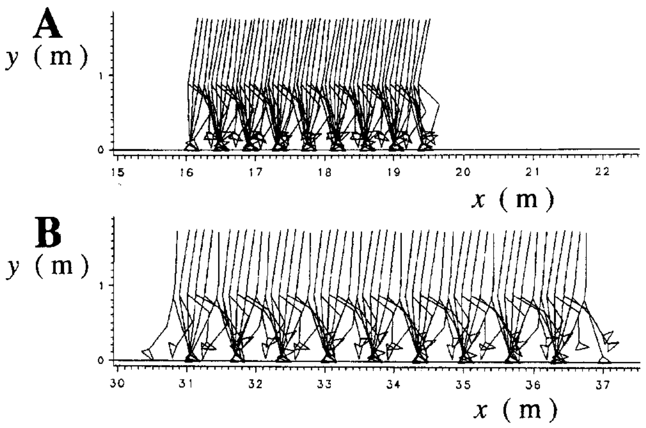

**Fig. 8A, B.** Control of walking speed by tonic input to the neural rhythm generator. Stick figures of walking at different speeds were traced every 0.09 s. **A** Slow walking, $u_0 = 5.0$; **B** fast walking, $u_0 = 7.0$

speed increased as the value of this parameter increased. Figure 8 shows typical examples of stick figures of walking movements at slow and fast speeds. Stable movements were obtained when $4.5 \leqslant u_0 \leqslant 7.0$. The fastest walking was almost twice as fast as the slowest walking.

As the value of this parameter was changed systematically, two different limit cycle attractors were revealed: one corresponding to a pattern of slow walking and the other corresponding to a pattern of fast walking. Figure 9A–C show the stride cycle duration, stride length, and speed as a function of the tonic input, respectively. Transitions between the patterns of slow and fast walking occurred discontinuously with hysteresis, although conspicuous changes were not observed in the pattern of neural activity, muscle torques, and displacements of the segments. This is in contrast to the bifurcation of walking and running patterns in a simple biped model (Taga et al. 1991). Figure 9D and E shows the stride cycle duration

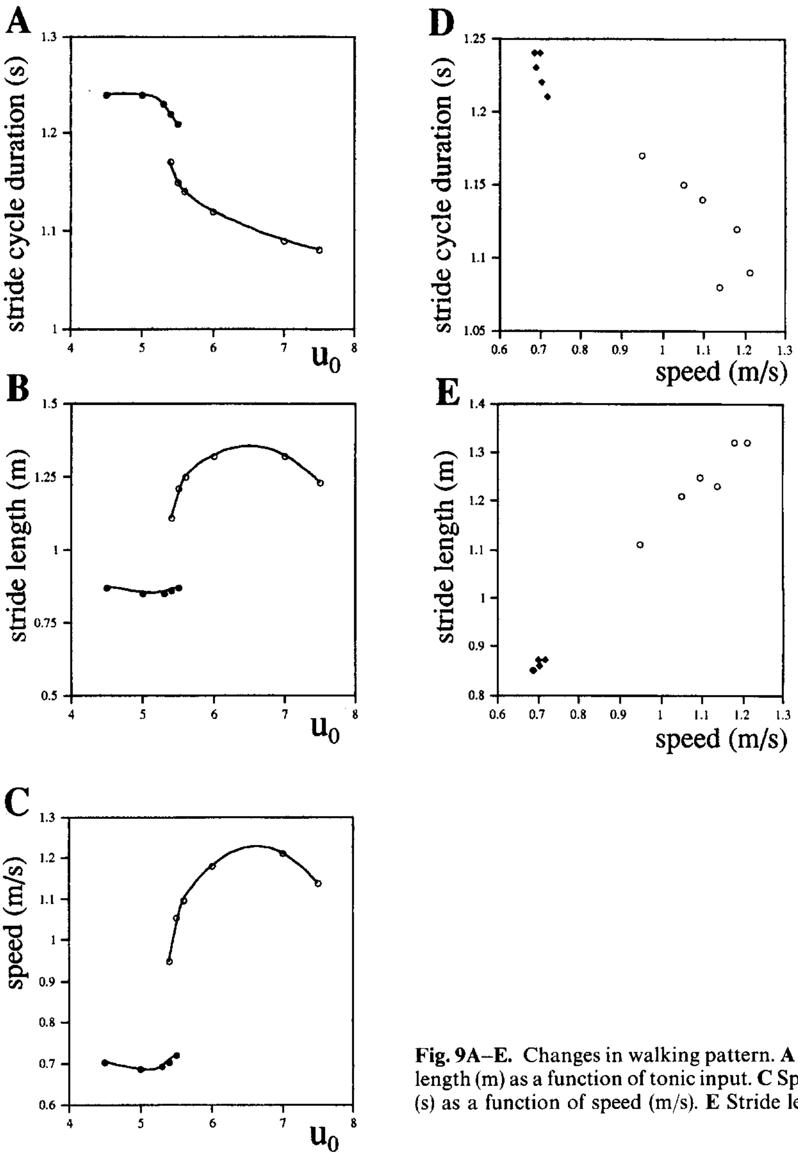

**Fig. 9A–E.** Changes in walking pattern. **A** Stride cycle duration (s) as a function of tonic input. **B** Stride length (m) as a function of tonic input. **C** Speed (m/s) as a function of tonic input. **D** Stride cycle duration (s) as a function of speed (m/s). **E** Stride length (m) as a function of speed (m/s) and length as a function of the walking speed, which are often measured in experiments of walking on a treadmill (Nilsson and Thorstensson 1987). The stride length showed a more conspicuous change than the stride cycle duration. Despite the discontinuous transition between the two states, the increase in the stride length and the decrease in the stride cycle duration as a function of the walking speed were monotonous. These relationships among the stride cycle duration, stride length and walking speed can be compared with those in human experiments, although there has been no report of two walking patterns being observed.

### *4.2 Entrainment of walking rhythm*

With regard to the control of the step cycle, we assumed that the higher center of the neutral system can generate rhythmic signals which are induced by the intention of stepping with a specific rhythm or which are induced by rhythmic information originating from visual, auditory, or other sensory signals. The rhythmic signals are then sent to the neural rhythm generator and entrain the stepping movement. In this model, sinusoidal signals were imposed on neurons in antiphase relationships between the flexor and extensor neurons and between the neurons on the right and left side. The signals imposed on each of the neurons of the hip oscillators on both sides can be written as

$$
\begin{aligned}
\tilde{u}_{0\text{right}-\text{hip}-\text{flexor}} &= -p\sin qt \\
\tilde{u}_{0\text{right}-\text{hip}-\text{extensor}} &= p\sin qt \\
\tilde{u}_{0\text{left}-\text{hip}-\text{flexor}} &= p\sin qt \\
\tilde{u}_{0\text{left}-\text{hip}-\text{extensor}} &= -p\sin qt
\end{aligned}
\qquad (6)
$$

where $p$ and $q$ are constant parameters that determine the amplitude and frequency of the sinusoidal signals, respectively.

When the frequency of the input signals was chosen appropriately, the stepping rhythm was entrained to the imposed rhythm, as shown in Fig. 10. When $p = 0.2$, absolute entrainment occurred when $5.3 \leqslant q \leqslant 5.7$. Note that $q = 5.6$ corresponds to the natural frequency of the walking movements. An imposed rhythm at slightly above or below the natural frequency can entrain the stepping rhythm. Since this behavior is a typical characteristic of a nonlinear oscillator, the entire system can be regarded as a single nonlinear oscillator. This further predicts that walking movements of two persons can be easily entrained through the interaction of rhythmic information. A simple model of synchronized stepping of two bipeds was previously demonstrated (Taga et al. 1993).

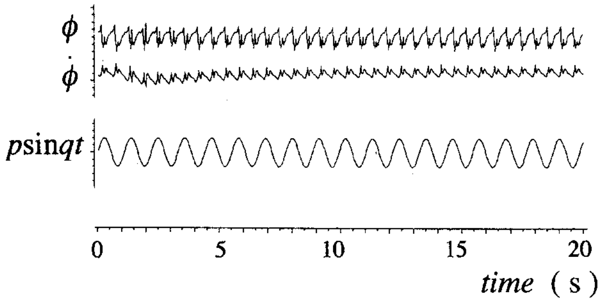

**Fig. 10.** Entrainment of stepping by rhythmic input to the neural rhythm generator; $p = 0.2$, $q = 5.7$

## 5 Discussion

We have demonstrated that the model is robust against various types of environmental changes and produces varieties of walking movements. Once we obtain steady walking on flat ground, adaptive walking under various constraints of an environment and tasks can be obtained without changing any internal structure of parameters. This extreme flexibility emerged from the property that all of the parts of the system interact directly or indirectly to form an attractor in the state space of both the musculo-skeletal and neural systems. The neural system of our model is designed to produce a basic pattern of muscle activation, which is established not only by the connections between the neural oscillators but also by the input of sensory signals representing body movements. The input pathway of the sensory information is chosen such that a phase locking occurs between the rhythmic activities of each neural oscillator and the rhythmic displacements of the global angle of the entire body, which corresponds to an unstable degree of freedom. Through this recurrent interaction in the sensorimotor loop, the instability of the human body is stabilized as a stable limit cycle. The amplitude and frequency of the rhythmic activity of the neurons, the magnitude of muscle torques and the trajectory of the limbs, etc., are determined depending on the environmental and task constraints. As long as the basic sequence of events that take place in the neuromusculoskeletal system is not changed by some changes in constraints, the stability of the attractor is maintained. Disturbances and changes that are given to a part of the system are compensated by the coordinated motion of the entire system. This type of stability and flexibility is completely different from that of a control system based on strict planning of a trajectory and a feedback controller which reduces deviation from the desired trajectory.

In human subjects, unexpected disturbances of a single limb during posture and locomotion induce well-organized responses of the muscles of the bilateral limbs (Berger et al. 1984; Dietz et al. 1989). These compensatory behaviors in real time can be compared with those of our model, in which the orbital stability of the limit cycle is established globally. Berger et al. (1984) also reported that the COG remained unaffected by perturbations. However, in this present model, stable walking movement is maintained even when the COG is strongly disturbed by perturbations, although there is a transient state of several step cycles before the steady-state is reached. The elucidation of transient behaviors in human subjects would be an important part of validating the control principle of this model.

Clark et al. (1993) showed that phase portraits of the motion of thigh and shank segments when subjects initiate walking from a standing position can be characterized as a stable limit cycle that is attracted to a specific region of the state space. Furthermore, the phase portraits of the same subjects with a mass affixed to their ankle retain stable shapes. These experiments, therefore, strongly support the notion that the adaptive movements of human walking take the form of attractors with orbital and structural stability, as demonstrated in our model.

In the present model, we have disregarded some points that may affect the stability of locomotion. First, it does not include the dynamics of muscles, which may improve the stability against perturbations. Soest and Bobbert (1993) examined the role of muscle properties in vertical jumping and showed that the muscle system works as a kind of feedback controller and reduces the effect of perturbations during execution, when no neural feedback is available. Second, incorporation of metatarsophalangeal (MP) joints of the foot may have a significant effect on the stability and controllability of the motion of the entire body. Miyazaki and Yamamoto (1993) showed that the maximum MP moment in normal level walking is as much as one-fifth to one-third of the maximum plantar flexion ankle joint moment. Although the MP moment during disturbed walking has not been reported, this moment may significantly increase the extent of stable walking.

Adaptability of locomotion under task constraints is related to the extent to which the basic locomotor pattern can be modulated. Humans unconsciously choose a specific combination of stride cycle duration and stride length at a given speed (Inman et al. 1981). Such preferred patterns of walking can be modulated voluntarily if required (Nilsson and Thorstensson 1987; Bonnard and Pailhous 1993). In this model, changes in the tonic input to the neural rhythm generator produce the specific frequency-amplitude relationship as a function of speed, which can be compared to that in human experiments, while the rhythmic input modulates the frequency of walking. Thus, the combination of tonic and rhythmic signals to the neural rhythm generator can generate a great variety of walking patterns depending on the task constraints.

It is an open question how adaptive locomotion is generated under more difficult situations like stair climbing and obstacle avoidance. To understand the mechanism of such anticipated adaptation, it is essential to know how signals that modulate the activity of the neural rhythm generator are generated in the brain depending on the task constraints, although we assumed that such signals are given and fixed in the present model. Schöner (1993) showed that motor control can be divided into three levels: the load level, at which effectors interact with external mechanical forces; the timing level, at which temporal order inherent to movement is generated; and the goal setting level. The description of the first and second levels corresponds to the body and neural dynamics of the present model, respectively. In this sense, our neural model should be extended to have dynamics of task goal setting. Drew (1988) showed that discharge of the motor cortex of cats modulated basic rhythm in the spinal central pattern generator and generated appropriate movements of the forelimb for intentional avoidance of obstacles during walking. It would be interesting to know how the discharge of the motor cortex is generated by visual information about obstacles, sensory information regarding limbs and the internal state of the spinal pattern generator. Integration of neurophysiological studies of locomotion and reaching behavior in animals (Georgopoulos and Grillner 1989; Kalaska and Drew 1993) may provide insight into the mechanisms of the anticipated control of locomotion in humans (Patla 1991). The present model may form a bridge between neurophysiology in animals and biomechanics in humans and provide general principles underlying adaptive control of human locomotion.

*Acknowledgements.* This research was supported by fellowships of the Japan Society for the Promotion of Science for Japanese Junior Scientists and by a Grant-in-Aid for Scientific Research (No. 2729) from the Ministry of Education, Science and Culture, Japan. I would like to thank Profs. H. Shimizu, Y. Yamaguchi, Y. Miyake, and M. Murase for their valuable comments.

## References

Beer RD (1990) Intelligence as adaptive behavior. Academic Press, London

Berger W, Dietz V, Quintern J (1984) Corrective reactions to stumbling in man: neuronal co-ordination of bilateral leg muscle activity during gait. J Physiol 357:109–125

Bonnard M, Pailhous J (1993) Intentionality in human gait control: modifying the frequency-to-amplitude relationship. J Exp Psychol Hum Percept Perform 19:429–443

Clark JE, Truly TL, Phillips SJ (1993) On the development of walking as a limit cycle system. In: Smith LB, Thelen E (eds) A dynamic systems approach to development: application. MIT Press, Cambridge Mass., pp 71–93

Dietz V (1992) Human neuronal control of automatic functional movements: interaction between central programs and afferent input. Physiol Rev 72:33–69

Doya K, Yoshizawa S (1992) Adaptive synchronization of neural and physical oscillators. In: Moody JE, Hanson SJ, Lippmann RP (eds) Advances in neural information processing systems 4. Morgan Kaufmann, San Mateo pp 109–116

Drew T (1988) Motor cortical cell discharge during voluntary gait modification. Brain Res 457:181–187

Ekeberg Ö (1993) A combined neuronal and mechanical model of fish swimming. Biol Cybern 69:363–374

Furusho J, Sano A (1991) Development of biped robot. In: Patla AE (ed) Adaptability of human gait. Elsevier Science, North-Holland Amsterdam, pp 277–303

Georgopoulos AP, Grillner S (1989) Visuomotor coordination in reaching and locomotion. Science 245:1209–1210

Grillner S (1985) Neurobiological bases of rhythmic motor acts in vertebrates. Science 228:143–149

Inman VT, Ralston HJ, Todd F (1981) Human walking. Williams & Wilkins, Baltimore

Kalaska JF, Drew T (1993) Motor cortex and visuomotor behavior. Exercise Sport Sci Rev 21:397–436

Kimura S, Yano M, Shimizu H (1993) A self-organizing model of walking patterns of insects. Biol Cybern 69:183–193

Matsuoka K (1985) Sustained oscillations generated by mutually inhibiting neurons with adaptation. Biol Cybern 52:367–376

Miura T, Shimoyama I (1984) Dynamic walk of a biped. Int J Robot Res 3:60–74

Miyazaki S, Yamamoto S (1993) Moment acting at the metatarsophalangeal joints during normal barefoot level walking. Gait Posture 1:133–140

Nilsson J, Thorstensson A (1987) Adaptability in frequency and amplitude of leg movements during human locomotion at different speeds. Acta Physiol Scand 129:107–114

Patla AE (1991) Visual control of human locomotion. In: Patla AE (ed) Adaptability of human gait. Elsevier Science, North-Holland, Amsterdam pp 55–97

Raibert MH (1984) Hopping in legged systems-modeling and simulation for the two-dimensional one-legged case. IEEE Trans SMC 143:451–463

Raibert MH, Hodgins JK (1992) Legged robots. In: Beer RD, Ritzmann RE, McKenna T (eds) Biological neural networks in invertebrate neuroethology and robotics. Academic Press, London, pp 319–354

Schöner G (1993) From interlimb coordination to trajectory formation: common dynamical principles. In: Swinnen S, Heuer H, Massion J, Casaer P (eds) Interlimb coordination: neural, dynamical, and cognitive constraints. Academic Press, London, pp 339–368

Schöner G, Kelso JAS (1988) Dynamic pattern generation in behavioral and neural systems. Science 239:1513–1520

Shik ML, Severin FV, Orlovsky GN (1966) Control of walking and running by means of electrical stimulation of the mid-brain. Biophysics 11:756–765

Soest AJ van, Bobbert MF (1993) The contribution of muscle properties in the control of explosive movements. Biol Cybern 69:195–204

Taga G (1994) Emergence of bipedal locomotion through entrainment among the neuromusculoskeletal system and the environment. Physica D 75:190–208

Taga G (1995) A model of the neuromusculoskeletal system for human locomotion. I. Emergence of basic gait. Biol Cybern 73:97–111

Taga G, Yamaguchi Y, Shimizu H (1991) Self-organized control of bipedal locomotion by neural oscillators in unpredictable environment. Biol Cybern 65:147–159

Taga G, Miyake Y, Yamaguchi Y, Shimizu H (1993) Generation and coordination of bipedal locomotion through global entrainment. Proc Int Symp Autonomous Decentralized Systems. IEEE Computer Society Press, pp 199–205

Takanishi A, Lim H, Tsuda M, Kato I (1990) Realization of dynamic biped walking stabilized by trunk motion on a sagittal uneven surface. IEEE Int. Workshop on Intelligent Robots and Systems, pp 323–330

Vukobratovic M, Stokic D (1975) Dynamic control of unstable locomotion robots. Math Biosci 24:129–157